

Control of Spin Defects in Wide-Bandgap Semiconductors for Quantum Technologies

Deep level defects found in diamond (nitrogen-vacancy center) and in silicon carbide (divacancy) have a quantum nature for the spins that manifests itself even at room temperature. These can be used as extremely sensitive nanoscale temperature, magnetic-field, and electric-field sensors. In the future, microwave, photonic, electrical, and mechanical control of these spins may lead to quantum networks and quantum transducers.

By F. JOSEPH HEREMANS, Member IEEE, CHRISTOPHER G. YALE, AND DAVID D. AWSCHALOM, Member IEEE

ABSTRACT | Deep-level defects are usually considered undesirable in semiconductors as they typically interfere with the performance of present-day electronic and optoelectronic devices. However, the electronic spin states of certain atomic-scale defects have recently been shown to be promising quantum bits for quantum information processing as well as exquisite nanoscale sensors due to their local environmental sensitivity. In this review, we will discuss recent advances in quantum control protocols of several of these spin defects, the negatively charged nitrogen-vacancy (NV^-) center in diamond and a variety of forms of the neutral divacancy (VV^0) complex in silicon carbide (SiC). These defects exhibit a spin-triplet ground state that can be controlled through a variety of techniques, several of which allow for room temperature operation. Microwave control has enabled sophisticated decoupling schemes to extend coherence times as well as nanoscale sensing of temperature along with magnetic and electric fields. On the other hand, photonic control of these spin states has provided initial steps toward integration into quantum networks, including entanglement, quantum state teleportation, and

all-optical control. Electrical and mechanical control also suggest pathways to develop quantum transducers and quantum hybrid systems. The versatility of the control mechanisms demonstrated should facilitate the development of quantum technologies based on these spin defects.

KEYWORDS | Diamond; divacancy; microwave; nitrogen-vacancy center; photonics; quantum control; silicon carbide; spin defects; wide-bandgap semiconductors

I. INTRODUCTION

Wide-bandgap semiconductors offer an excellent platform as a host material for atomic-scale defects with highly localized electronic states that are optically addressable, have nonzero spin ground states, and share similar properties to those of trapped atoms. These spin defects, often referred to as color centers, have garnered great interest over the past few decades as a viable resource for quantum information processing and nanoscale sensing applications. The unique properties of these defect states allow for a wide array of control mechanisms including microwave, photonic, electrical, and mechanical manipulation.

At their core, the spin states of these solid-state defects are promising candidates to fulfill the DiVincenzo criteria as quantum bits, or qubits. These criteria summarize the basic requirements for a viable qubit needed for quantum information processing. These properties include the ability

Manuscript received November 2, 2015; revised April 11, 2016; accepted April 17, 2016. Date of publication May 24, 2016; date of current version September 16, 2016. F. J. Heremans and D. D. Awschalom are with the Institute for Molecular Engineering, University of Chicago, Chicago, IL 60637 USA, and also with the Materials Science Division, Argonne National Laboratory, Argonne, IL 60439 USA (e-mail: awsch@uchicago.edu). C. G. Yale is with the Institute for Molecular Engineering, University of Chicago, Chicago, IL 60637 USA.

Digital Object Identifier: 10.1109/JPROC.2016.2561274

0018-9219 © 2016 IEEE. Translations and content mining are permitted for academic research only. Personal use is also permitted, but republication/redistribution requires IEEE permission. See http://www.ieee.org/publications_standards/publications/rights/index.html for more information.

to initialize and read out the qubit's state, a universal series of quantum gates, and a long coherence time of the qubit state relative to these quantum operations [1]. While these defects may be relevant toward the long-term development of quantum computing, they also show promise to realize other quantum technologies, including quantum repeaters and nanoscale sensors.

This review will discuss recent developments in quantum control mechanisms of spin defects and how they might be combined to harness complex quantum systems for use in quantum networks and as nanoscale sensors. Quantum networks and repeaters are envisioned as a way to transfer quantum information among stationary qubit nodes through flying qubits (photons), and may be thought of as the quantum equivalent of today's fiber optics and amplifiers. The electronic spin of these defects also possesses a strong sensitivity to their local environment, enabling their utility as nanoscale sensors of magnetic [2] and electric fields [3], as well as temperature [4]. Another interesting application is to transfer the electron spin state to a nearby nuclear spin, resulting in a "quantum memory" [5], [6] that can be written and then read out at a later time. While there is significant research into developing nuclear memories and registries [7]–[11], we will not focus on those approaches in this review, and instead focus on the diverse methods to control the electronic spin state of a single defect and how this wide palette of control enables the development of quantum technologies.

II. SPIN DEFECTS IN WIDE-BANDGAP SEMICONDUCTORS

A. Criteria for Suitable Defect Spins

The archetypal optically addressable spin defect is the negatively charged nitrogen-vacancy (NV^-) center in diamond (see Section II-C) [12]–[14], and there have also been recent efforts to identify several other potential defects of interest. This includes other defects in diamond, such as the silicon-vacancy center ($V-I_{Si}-V$) [15]–[17], which is promising for photonic applications due to most of its emission occurring within the zero-phonon line. Efforts have also focused on defects arising in technologically more mature materials (see Section II-D), such as in silicon carbide (SiC), including the silicon-site vacancy (V_{Si}) [18], [19], a variety of forms of the neutral divacancy (VV^0) [20]–[23], and carbon antisite vacancies ($C_{Si}V_C$) [24], as well as in zinc oxide (ZnO), where single photon emitters have been detected [25]. To identify other potential defects that are similar to the NV^- center in diamond, Weber, Koehl, Varley *et al.* (WKV) consolidated a generalized criteria for optically addressable defects [26], which postulate that a suitable defect have the following characteristics:

- consists of bound states that have energy gaps large enough to avoid thermal excitation;

- has an optical pumping cycle that polarizes the qubit state;
- emits luminescence that is dependent on the qubit state in some differentiable way;
- contains optical transitions that do not interfere with the electronic states of the host material.

B. The Intersystem Crossing

The second and third criteria can be described as optical addressability, and in the case of several of the aforementioned defects (in particular, the diamond NV^- and the SiC VV^0), it stems from a level structure that allows for spin-dependent intersystem crossings (ISCs), enabling both optical spin initialization and readout of the spin state based on photoluminescence (PL). An intersystem crossing is a nonradiative process between two electronic spin states of different spin multiplicity [see Fig. 1(c)] and allows for an alternate pathway between the excited state (ES) and the ground state (GS).

Both of these defects of interest have two-electron states that comprise a combination of spin-triplet and spin-singlet levels with largely spin-conserving transitions between them [14]. In these defects, the lowest lying level (the ground state) is spin triplet in nature, $S = 1$ with quantum numbers $m_s = -1, 0, +1$. The $m_s = 0$ and $m_s = \pm 1$ sublevels are naturally split due to the crystal field splitting (D), and the $m_s = \pm 1$ can be split through application of an external magnetic field. The excited state is also spin triplet in nature [14], and the presence of this ISC allows the spin to pass between the spin-triplet and spin-singlet levels, facilitating the quantum control of these defects [see Fig. 1(c)]. For certain spin defects, such as the NV^- center, this control extends even beyond room temperature [4].

Initialization occurs when driving an optical cycle from the GS to the ES that can decay through the ISC with a certain preferential probability depending on the initial spin state. Repeatedly driving these transitions ultimately initializes the system into the spin state that does not preferentially undergo intersystem crossing. Likewise, the amount of light emitted is spin dependent. This is because the state that preferentially couples through the ISC yields a reduction in photon emission due to the fact that pathways accessed by ISCs are significantly less radiative. The resulting PL contrast acts as a readout of the spin state of the defect.

C. The Nitrogen-Vacancy Center in Diamond

The negatively charged nitrogen-vacancy (NV^-) center is a paramagnetic defect within the diamond lattice which consists of a substitutional N impurity adjacent to a vacant lattice site [see Fig. 1(a)] [12]. Within this defect complex, there are a total of six electrons, highly confined within the nitrogen atom and vacancy dangling bonds [27], [28]. The resulting level structure has an optical transition of ~ 1.945 eV, which is situated well within the

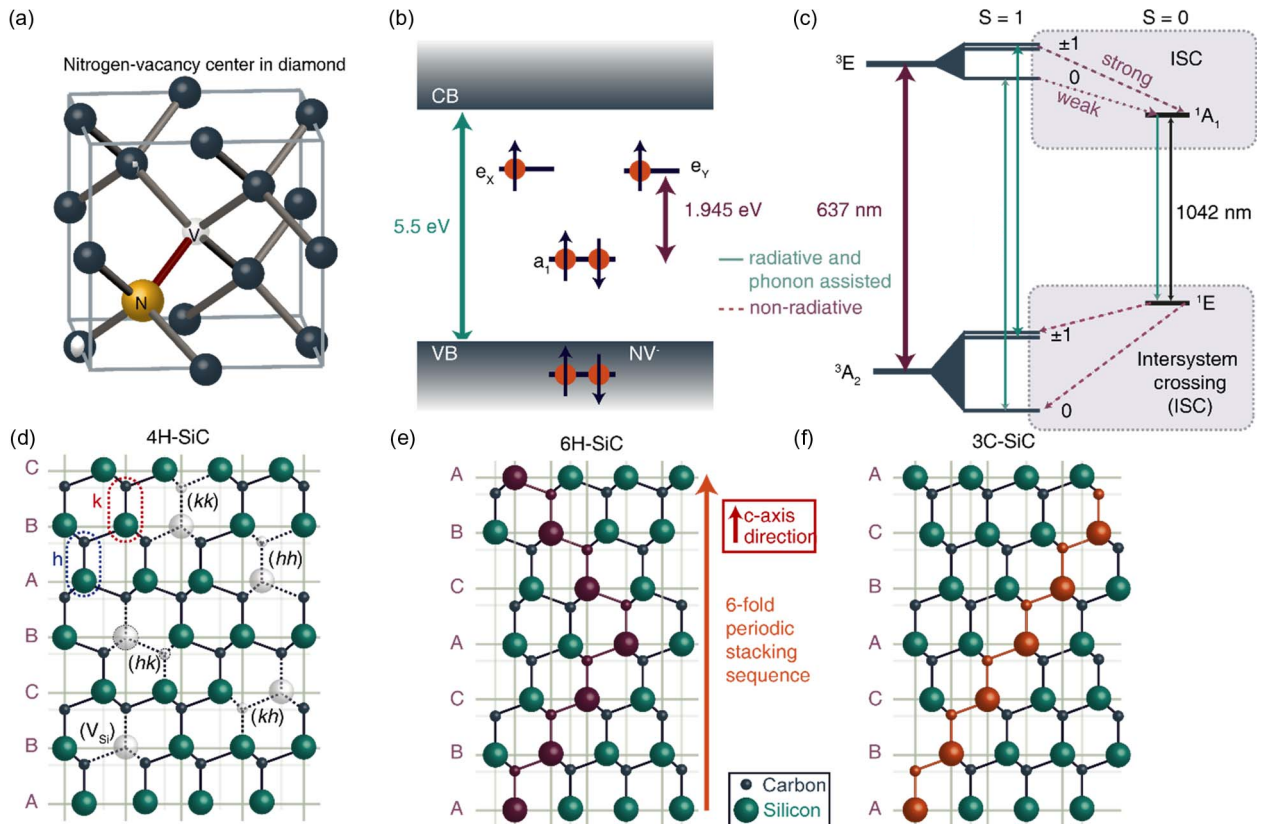


Fig. 1. Crystal and level structure of common spin defects. (a) The crystal structure of a negatively charged nitrogen-vacancy (NV⁻) center in diamond. It comprises a substitutional nitrogen defect adjacent to a lattice vacancy. (b) The electronic energy levels of the NV⁻ center in its spin ground state configuration comprising six total electrons, two in the valence band, two paired in the a₁ state and one each in the e_y and e_x states. The level structure is well isolated within the much larger 5.5-eV bandgap of diamond. (c) A detailed level structure of NV⁻ center spin system showing the direct zero-phonon line optical transition (~637 nm) as well as the ISC. The ISC plays a crucial role in the spin-dependent photoluminescent readout, as well as optical initialization of the spin state as described in the text. (d) The crystal structure of 4H-SiC along with the various basal (hk and kh) and c-axis (hh and kk) divacancy complexes and the silicon-site vacancy (V_{Si}). (e) The crystal structure of 6H-SiC. Note the sixfold stacking sequence periodicity. (f) The crystal structure of 3C-SiC, a zincblende crystal structure very similar to the diamond lattice.

much larger 5.5-eV bandgap of the diamond crystal lattice [see Fig. 1(b)] [29]. This isolation within the bandgap and its localized wavefunction, along with low spin-orbit coupling and the high Debye temperature of diamond enable the NV⁻ center to have remarkable spin coherence times up through room temperature [30] extending above $T > 600$ K [4]. The $m_s = \pm 1$ states of the ES also preferentially couple through the ISC [see Fig. 1(c)] enabling optical initialization into $m_s = 0$ and spin-dependent PL readout. These features have made the NV⁻ center a convenient testbed for exploring quantum control and developing quantum technologies in the solid state.

The wide array of control mechanisms discussed in this review, including microwave, optical, and mechanical techniques, have made the NV⁻ center one of the vanguards of quantum information science. The NV⁻ center was recognized early on as a qubit for applications in quantum information processing, toward the development of quantum repeaters and quantum communication [31]. In such a

scheme, the NV⁻ center's electronic and nuclear states would act as the stationary nodes, allowing for memory operations (entanglement swapping and state purification). These individual nodes would be coupled with photons to transmit and teleport information. Numerous efforts have realized entanglement between NV⁻ center spins and photons [32], [33], two NV⁻ center spins through dipolar coupling [34], two NV⁻ centers photonically [35], as well as teleportation of the spin state of one NV⁻ center to another [36]. In addition to its role in developing quantum information processing, the NV⁻ center's sensitivity to its local environment makes it an excellent nanoscale sensor [2]–[4], [37]–[41].

D. Beyond Diamond—The Divacancy in Silicon Carbide

Due to the growing interest in the NV⁻ center as a versatile platform for quantum technology, recent efforts have been made to explore optically addressable defects

in materials other than diamond [26], including silicon carbide [21] and zinc oxide [25]. Such materials are promising, as they meet a series of criteria again formulated by WKV [26] which describe the ideal spin defect host material. These WKV criteria call for a material that has:

- a wide bandgap;
- small spin-orbit coupling;
- nuclear spin-free lattice;
- availability of high-quality bulk or thin-film single crystal.

These criteria are not exclusive, but rather guidelines toward identifying materials that may have NV^- center analogs.

Specifically, SiC has been a material of great interest as it is prevalent in the semiconductor industry for high-power electronics and MEMS sensors. This technological maturity of SiC as an electronic grade semiconductor allows for development of optoelectronics that can be leveraged to produce sophisticated devices. Whereas monocrystalline diamond of suitable quality for defect spin studies must be specially grown on the millimeter length scale, high-quality commercial SiC, available up to 6" wafer sizes, has been demonstrated as a sufficient defect host material. In addition, SiC is a compound semiconductor with over 200 polytypes, or different atomic stacking configurations forming the crystal structure [see Fig. 1(d)–(f)]. This results in numerous symmetry configurations leading to a variety of defect orientations, bandgaps, and other physical properties. Thus far, experiments have investigated spin defects in the 3C, 4H, and 6H polytypes of SiC.

Among these defects in SiC, neutrally charged divacancy complexes (VV^0) have recently emerged as an excellent analog to the NV^- center [20], [21], [42]–[44] and have very recently been isolated at the single spin level [23]. These complexes come in four different inequivalent lattice configurations in 4H-SiC [see Fig. 1(d)] referred to as hh , kk , hk , and kh (PL1-4, respectively, according to [21]), which persist up to $T \sim 200$ K. Other polytypes offer a suitable host as well, and their stacking sequence determines the number of distinct lattice configurations of the VV^0 . For instance, in 6H-SiC [Fig. 1(e)], there are six divacancy configurations, while in 3C-SiC [Fig. 1(f)], only one configuration exists [22]. While investigations are ongoing, several of these configurations, as well as some unidentified defects, have shown persistence up to room temperature.

It is worth noting that both of the defects discussed in this review are found in a host material which has a nominally nuclear spin-free lattice and follow the WKV criteria. While there may still be some natural isotopic abundance of ^{13}C (1.07%) and ^{29}Si (4.67%) that cause decoherence due to their nuclear spins, the spin coherence times of these defects are still remarkably long [45]. In particular, while SiC has significantly more nuclear spins than diamond, the electronic spin states, such as those in the V_{Si} , still have long coherence times that depend strongly on

the external magnetic field [46], [47]. The removal of nuclear spin impurities through special growth of isotopically pure materials has been shown to increase the spin coherence time of the NV^- center in diamond from hundreds of microseconds to ~ 2 ms [30]. Ultimately, these spin coherence times will be limited by the electron spin-lattice relaxation time (T_1), which is a few milliseconds for NV^- center ensembles at $T = 300$ K [48].

It is possible to find spin defects in host materials that do not fully conform to the WKV criteria, such as materials that lack a spin-free lattice, but this may decrease the spin coherence time and ultimately the practicality of these spin defects. In materials with very specific properties (e.g., piezoelectric, strong coupling to other quantum systems, or promising photonic materials) these spin defects may still provide interesting research avenues for technological application.

III. MICROWAVE CONTROL OF GROUND STATE SPIN

A. Optically Detected Magnetic Resonance in Defect Spins

To observe and manipulate these spin defects, the typical approach is through the use of a confocal microscope, where the defect is excited resonantly, or non-resonantly within its absorption band, and its PL is collected with a single-photon detector [13], [19], [23]. As previously mentioned, several of these defects are controllable beyond room temperature, but some quantum control characterizations do require the use of an optical cryostat to reach cryogenic temperatures.

In particular, the NV^- center emits PL with a spectrum [see Fig. 2(a)] that consists of a 1.945-eV (637-nm) zero phonon line (ZPL), the direct energy transition between the ground and excited states, as well as a phonon-assisted emission sideband extending out to ~ 1.55 eV (800 nm). The phonon-assisted absorption sideband similarly extends to higher energies allowing for off-resonant excitation of the spin defect. In the case of NV^- centers, 532-nm (2.33-eV) excitation is commonly used. However, exciting along the 575-nm (2.16-eV) ZPL of the neutrally charged nitrogen-vacancy center (NV^0) aids in the stability of the NV^- center [49], while exciting at 590 nm (2.10 eV) may be used to avoid the excitation of the other charge state altogether [50]. The charge stability of the electrostatic environment stems from other defects that are optically excited within the laser spot size.

The most common way to manipulate the NV^- center electronic spin state is through use of optically detected magnetic resonance (ODMR), a technique that is the optical equivalent of electron spin resonance (ESR) or nuclear magnetic resonance (NMR), where the signal contrast results from spin-dependent PL. An ODMR measurement uses microwave frequencies to drive an

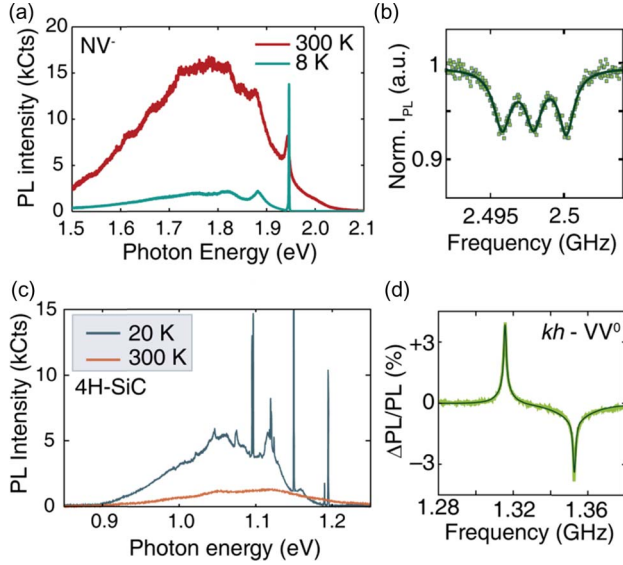


Fig. 2. PL spectra and optically detected magnetic resonance. (a) The PL spectra of an NV^- center at room temperature and cryogenic temperatures. The zero-phonon line is very sharp at cold temperatures, while the phonon sideband is much more prominent at room temperature. (b) The optically detected magnetic resonance (ODMR) signal for an NV^- center showing the resonance transition between the $m_s = 0 \Leftrightarrow m_s = -1$ transition at an external magnetic field of $B \sim 115$ G. The three dips result from the hyperfine coupling of the intrinsic ^{14}N atom. Adapted from [51]. (c) The PL spectra of divacancy defects in 4H-SiC silicon carbide at room temperature and cryogenic temperatures ($T = 20$ K). Adapted from [21]. (d) The ODMR signal of an ensemble of $kh - VV^0$ (PL4), one of the divacancy complexes in 4H-SiC. Adapted from [21].

oscillating AC magnetic field perpendicular to the NV^- center spin quantization axis to coherently manipulate the ground state spin triplet between $m_s = 0$ and $m_s = \pm 1$ spin states. At zero field, the $m_s = 0$ and $m_s = \pm 1$ are naturally split by a crystal field splitting of 2.87 GHz. Applying an external magnetic field along the NV^- center axis splits the zero-field degeneracy of the $m_s = \pm 1$ spin state at a rate of ~ 2.8 MHz/G. Thus by combining control of the external magnetic field and tuning the microwave frequency into resonance with a particular transition, a qubit state within the ground state spin triplet can be individually addressed and manipulated. In Fig. 2(b), we present the ODMR signal of a NV^- center at ~ 115 G on resonance with the $m_s = 0 \Leftrightarrow -1$ transition. The observation of three dips in PL is due to the hyperfine coupling of the ^{14}N (total spin $I = 1$) intrinsic to the NV^- center.

The various VV^0 configurations in SiC present similar photoluminescence [see Fig. 2(c)] and ODMR signatures. In any given polytype, each configuration will have a slightly different zero-phonon line (1.09–1.20 eV), along with a phonon-assisted emission sideband, extending out to 0.9 eV [22]. In certain cases, such as kh configuration of the VV^0 , both a dip and a peak are observed in

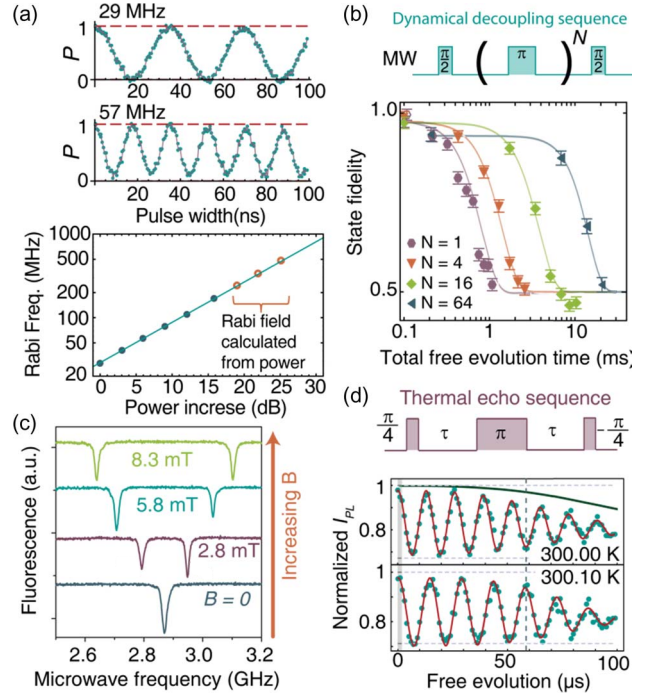


Fig. 3. Rabi oscillations and spin coherence in diamond. (a) Upper graphs: Rabi oscillations of an NV^- center at two different microwave powers resulting in Rabi oscillations of 29 and 57 MHz. Lower graph: the dependence of Rabi frequency on microwave driving power. Figure adapted from [54]. (b) Dynamical decoupling sequence and corresponding data extending the spin coherence time of the NV^- center by adding more refocusing π pulses to account for higher frequency fluctuations in the local environment. Adapted from [35]. (c) ODMR response to an external magnetic field demonstrating the sensitivity the NV^- center has to the local magnetic environment. Adapted from [37]. (d) The thermal echo sequence along with corresponding data taken at two different temperatures. This thermal echo greatly improves the thermal sensitivity of the NV^- center to around $10 \text{ mK}/\sqrt{\text{Hz}}$. Adapted from [39].

ODMR [see Fig. 2(d)], suggesting there exist different dynamics with regard to the intersystem crossing and spin polarization. Thus far, ODMR has been observed in the 4H, 6H, and 3C forms of SiC [22].

B. Rabi Oscillations in Diamond

Applying microwave pulses resonant with a ground state transition, and varying the pulse duration, induces Rabi oscillations [52] of the electron spin state, which are optically detected via the spin-dependent PL. Driving Rabi oscillations of the electron spin state allows for full inversion of the spin state as well as the ability to form any superposition (or mixture) of the two states. In Fig. 3(a), we show a Rabi oscillation between the $m_s = 0 \Leftrightarrow -1$ transition. A full inversion of the spin state, known as a π pulse [see Fig. 3(a)], results in a flip of the qubit state, while a $\pi/2$ pulse refers to a pulse that transfers the population of the $m_s = 0$ and $m_s = -1$ spin

states into an equal superposition, $(|0\rangle \pm |-1\rangle)/\sqrt{2}$, of those states.

Now a standard part of the repertoire for controlling these spin defects, Rabi oscillations in diamond NV^- centers were first observed by Jelezko *et al.* in 2004 [53], yielding coherent control of the ground state spin. Within the rotating frame of the microwave frequency resonant with the ground state energy separation (the Larmor precession frequency), these oscillations can be seen as a rotation about an equatorial axis on the Bloch sphere. Therefore, when the Rabi oscillation frequency is on the order of the Larmor frequency, the rotating wave approximation begins to break down, and careful pulse shaping is needed to achieve Rabi oscillation frequencies as high as 500 MHz [54], [55].

C. Probing Spin Coherence in Diamond

We can use the π and $\pi/2$ pulses determined by the Rabi oscillations to probe the spin coherence times of the NV^- center. These times reveal how long the spin state of the NV^- center retains its phase and state information before being lost to fluctuations in the environment, and so they act as a window in which a number of operations can be performed. The most basic coherence time is the free evolution time, or T_2^* , which is measured by placing the spin in a superposition, waiting a certain amount of time, and then projecting the resulting spin state [56]. This T_2^* effectively characterizes how long the spin remains coherent before fluctuations in the local environment destroy the phase information. A Hahn echo sequence removes the influence of slow fluctuations by applying a refocusing π pulse halfway through the sequence [57], effectively reversing the direction of phase accumulation [see Fig. 3(b) where $N = 1$ for pulse sequence]. These echo experiments characterize what is known as the T_2 coherence time.

The principles behind the Hahn echo sequence can be further extended by increasing the number of refocusing pulses and shortening the free evolution time between each pulse, which can extend the effective decoherence time by mitigating effects due to increasingly faster local fluctuations [see Fig. 3(b)] in a process known as dynamical decoupling [58], [59] with T_2 times reaching close to a second [60]. As the coherence time of the spin state is an important figure of merit for the practical implementation of these spin defects, extending this time maximizes the number of spin manipulations achievable per spin coherence time. This extended coherence facilitates quantum information protocols [61] and improves the sensitivity of the defect for metrology applications. While dynamical decoupling schemes are one method of prolonging the spin coherence time, material science efforts have also extended T_2 spin coherence times to the millisecond timescales in the NV^- center by using isotopic ^{12}C growth techniques to effectively eliminate the nearby ^{13}C nuclear spins [30], [62].

D. Nanoscale Sensing Applications

With this microwave control of the NV^- center spin state, a particularly fruitful avenue of research focuses on using the NV^- center as sensor of its local nanoscale environment. In particular because the NV^- center sublevels can be tuned by a magnetic field, their separation acts as a sensor of the local magnetic environment [37], [38]. Based on this principle, probing the sublevel separation measured through ODMR [see Fig. 3(c)] allows for the mapping of magnetic fields with ~ 20 nT/ $\sqrt{\text{Hz}}$ sensitivity [63], [64]. Sophisticated pulse schemes have been developed to improve sensitivity [65] enabling a wide array of applications [66] including nanoscale nuclear magnetic resonance [67], [68], magnetic imaging of cells [69], [70], and imaging of the magnetic moment of a proton [71]. In addition, techniques based on the sensitivity of T_1 relaxation have enabled the sensing of external gadolinium ion spins [72], [73] as well as substitutional nitrogen (P1 centers) within the diamond lattice [74].

More recently, the NV^- center has been demonstrated as a viable nanoscale thermometer. This is based on a temperature-dependent shift of the crystal field splitting D , measurable by ODMR, that results from a combination of the diamond lattice thermal expansion and electron-phonon interactions [4], [75], [76]. This technique reveals the NV^- center remains coherent with a thermal sensitivity of around 100 mK/ $\sqrt{\text{Hz}}$ at temperatures in excess of 600 K [4]. Through a pulse sequence known as a thermal echo, in which the $\pi/2$ pulses are replaced with $\pi/4$ pulses, the dependence of the spin sublevel splitting on magnetic field can be eliminated, revealing solely the temperature dependence of the crystal field splitting, and improving sensitivity to 1–10 mK/ $\sqrt{\text{Hz}}$ [39]–[41] [see Fig. 3(d)].

E. Geometric Control

An alternative method to controlling the ground state spin is to exploit geometric control, that is control based upon the accumulation of geometric phases. Such phases arise from cyclic evolution of a quantum mechanical system and are determined by the geometry of the region enclosed within parameter space. This is in contrast to the previously discussed control techniques which rely on dynamic phases, where control is determined by the time and energy of the interaction. In the case of NV^- centers, geometric control has been realized using microwaves to drive both magnetic-dipole transitions within the ground state in a V configuration. Typically, the evolution must be adiabatic in order to accumulate these phases, known as Berry phases, but certain degeneracies within the system allow for more general non-Abelian geometric phases, or holonomies. In the NV^- center, Berry phase has been measured and controlled by adiabatically evolving the control microwave fields [77] or optical fields [78]. Holonomic gates have also been

demonstrated in NV^- centers, leading to a universal set of qubit gates [79], [80] as well as the realization of a controlled-NOT (CNOT) gate by coupling to the intrinsic nitrogen nuclear spin [79]. Geometric control represents a more robust form of control as it is insensitive to the energetics or time of the interaction, as well as to certain types of noise [78], [81], [82]. As such, it represents a promising avenue for fault-tolerant quantum information processing.

F. Spin Coherence in SiC

Some of these microwave control techniques have recently been applied to manipulate the ground-state spin sublevels of various divacancies orientations in the SiC. ODMR, Rabi oscillations, and spin coherence measurements were demonstrated in ensembles of VV^0 complexes (hh , kk , hk , kh) in 4H-SiC at $T < 200$ K as well as with unknown defects (PL5 and PL6) that have a similar structure and persist up to room temperature [21]. More recently, these VV^0 complexes have been isolated at the single defect level [see Fig. 4(a)] exhibiting Rabi oscillations as fast as ~ 10 MHz corresponding to a π pulse of ~ 50 ns [see Fig. 4(b)]. These VV^0 defects exhibit spin coherence times (T_2) in excess of 1.2 ms, without any isotopic engineering of the host lattice or dynamical decoupling sequences [23].

Furthermore, by exploiting the inequivalent lattice sites, one species of VV^0 (drive species) can be manipulated in order to alter the Larmor precession of a second VV^0 (sense) species in 6H-SiC via double-electron-electron-resonance (DEER) [22]. These DEER measurements reveal the magnetic dipole coupling among different spin species within an ensemble, providing an intrinsic means of transferring quantum information [see Fig. 4(c)]. These advances are significant as SiC is a technologically more mature material and provides pathways toward integration of spin defects with more conventional semiconductor technology, as well as with photonics and mechanical motion.

IV. OPTICAL CONTROL OF DEFECT-BASED SPINS

A. Excited State Structure of the NV Center in Diamond

Due to the rich structure of the NV^- center excited state and its inherent optical addressability, the NV^- center has become an excellent testbed for a number of quantum optical protocols aimed at the development of photonic networks and quantum repeaters for quantum information processing [83]. Photonic control of the NV^- center exploits the excited state level structure of the NV^- center, consisting of six spin-orbit levels at zero magnetic and electric field. These orbital components are strongly susceptible to intrinsic strain and local

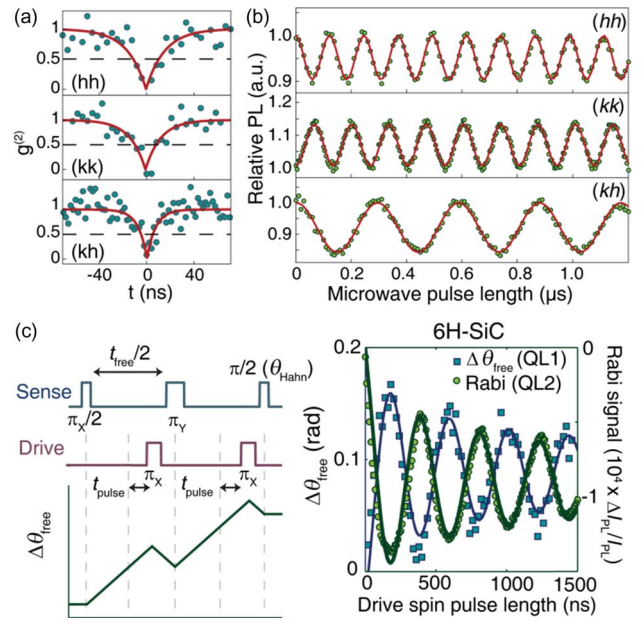


Fig. 4. Microwave control in VV^0 in SiC. (a) Single defects in SiC. The $g^{(2)}$ coherence function in a Hanbury-Brown-Twiss measurement reveals isolation of single VV^0 of several different configurations, the hh , kk , and kh species within 4H-SiC. (b) Corresponding Rabi oscillations driven in each of those individual single spins. Figures (a) and (b) from [23]. (c) Double-electron-electron-resonance (DEER) measurement on two ensemble species of VV^0 in 6H-SiC. Left: Pulse sequence to drive one species, and sense the Larmor precession of the other. Right: Variation of the pulse duration drives Rabi oscillations on the drive species (QL2) and accumulates DEER signal on the sense species (QL1). Figure from [22].

electrostatic fields, and can be tuned through the DC Stark effect either through additional applied strain or an external electric field [84]–[87]. Likewise, its spin components can be tuned through the Zeeman effect with an external magnetic field. As such, at high magnetic and electric fields, these levels split into a distinct orbital doublet E_X and E_Y , with each orbital containing a spin triplet. A more detailed treatment of the excited state can be found in [14] and [88]–[91].

This detailed structure of the ES is only optically resolvable at cryogenic temperatures ($T < 20$ K) [90], above which Jahn–Teller distortions cause significant broadening of these levels [92]. The room temperature operation of the NV^- center is enabled by an averaging process that leads to an orbital singlet-like ES with a spin triplet [93]. At cryogenic temperatures, the sharpening of the linewidth of these optical transitions facilitates on-resonant excitation, while the broadened ES at room temperature limits most applications to off-resonant excitation.

To resolve these levels at cryogenic temperatures, a tunable, narrow-line 637-nm laser is used to scan across the various transitions between the GS and ES,

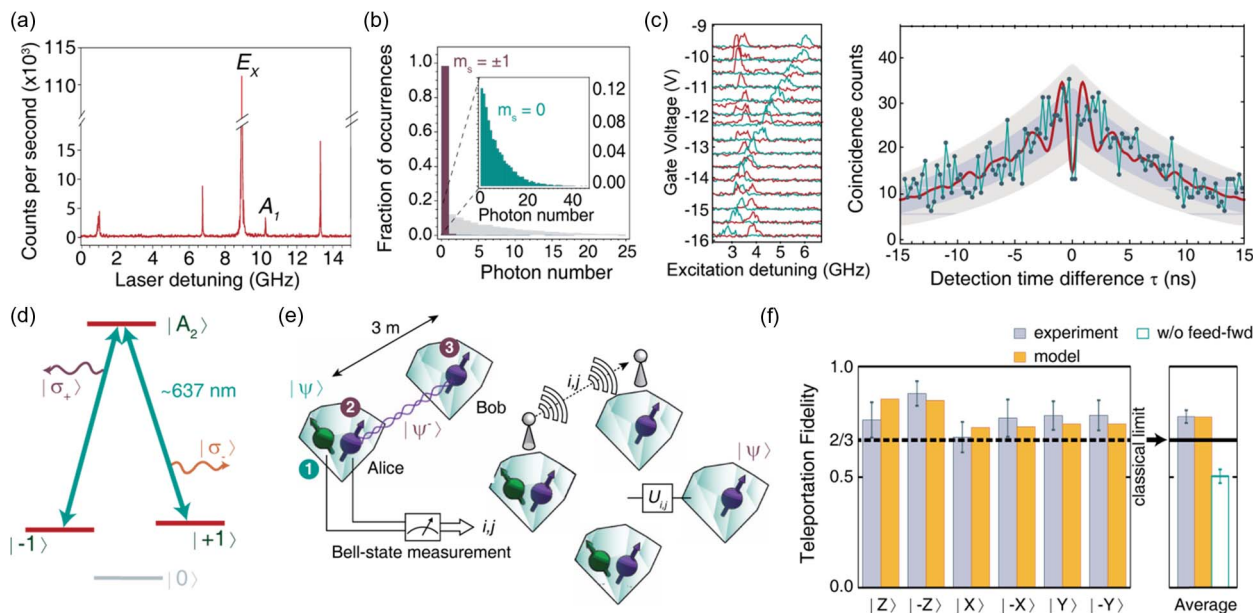


Fig. 5. Linking spins with light. (a) Photoluminescence excitation (PLE) of the NV^- center taken at cryogenic temperatures. The peaks correspond to the tunable, narrow-line laser being resonant with a specific GS \leftrightarrow ES transition. Figure from [95]. (b) The principles behind single-shot readout. Photon count statistics of the readout of the spin state during an optical pulse resonant with the E_x transition over 10000 measurement iterations. When initialized into $m_s = \pm 1$, the average photon count per shot is 0.07, and when initialized into $m_s = 0$, the average photon count per shot is 6.4. Figure adapted from [95]. (c) Two-photon interference from distinct NV^- centers. Left: By applying a voltage to the sample, the E_x transitions within two NV^- centers are brought to resonance around -13.6 V. Right: Coincidence distribution of 255 one-minute histograms. The dark and light gray regions denote the standard deviations (σ and 2σ) of the expectation for two noninterfering sources, while the red curve depicts a simulation of the expected behavior for interfering sources. Figure adapted from [98]. (d) The A_2 Λ system within the NV^- center. At zero field, the A_2 excited state couples to the $m_s = \pm 1$ ground states through orthogonal circular polarizations of light. Through this distinct coupling, spin-photon entanglement has been realized both for an emitted photon [32], as well as an absorbed photon [33]. (e) Depiction of teleportation of a spin state from one NV^- center to a distant NV^- center. Alice wishes to teleport qubit state ①. Alice and Bob both have one qubit of an entangled pair (qubits ② and ③). To teleport the state of qubit ①, Alice jointly measures qubits ① and ② in the Bell basis, thus projecting the state of qubit ① onto the state of qubit ③ up to a unitary transformation. This transformation depends on the outcome of Alice's measurement, and is transmitted to Bob classically. Bob then applies the unitary transformation, recovering the teleported state, which now resides on qubit ③. (f) The teleportation fidelity for six different initial states. The horizontal dashed line denotes the classical limit. Figures (e) and (f) adapted from [36].

measuring the emitted PL. Peaks appear when the laser is resonant with a specific transition [see Fig. 5(a)], in a measurement known as photoluminescence excitation (PLE) [90], [94]. These transitions are spin dependent [85] and provide another means of spin-state readout [95]. It should be noted that in most samples, these peaks are broadened beyond the transform limited linewidth as a result of spectral diffusion [92]. This diffusion occurs when charge instabilities around the NV^- center reset during certain types of photoexcitation, particularly that of the 532-nm off-resonant laser [96], [97], causing slight shifts in the electrostatic environment which are sensed by the NV^- center resulting in shifts of the optical transition energies. Over a series of measurements with repeated reinitializations by a 532-nm laser, this leads to a spectrally broadened peak [92]. However, with reionizations along the NV^0 zero-phonon line at 575 nm, the linewidth of the NV^- center optical transitions becomes transform limited [49].

Fabrication of a solid immersion lens coupled with a high numerical aperture objective within the cryostat leads to significant enhancement of the collection efficiency of the emitted PL [99], [100]. When exciting along specific spin-dependent transitions, this yields high-fidelity single-shot readout of the NV^- center spin state [95] [see Fig. 5(b)]. Likewise, by optically pumping the spin from one spin state to another, it is possible to initialize the spin state of the NV^- center with a greatly enhanced fidelity of 99.7% [95]. In addition, resonant excitation allows for the observation of optical Rabi oscillations between the ground and excited states, providing a way to fully populate the excited state of the NV^- center [101].

B. Linking NV Centers With Light

One of the most fascinating aspects of quantum mechanics is the entanglement of quantum states, a phenomenon by which multiple quantum states cannot be described independently but only as a whole system.

This gives rise to nonclassical correlations among the quantum states. The NV⁻ center was used in one of the first demonstrations of spin-photon entanglement in the solid state, as a particular sublevel of the ES (the A₂ level) couples to two GS spin states through different circular polarizations of light [see Fig. 5(d)], such that the polarization of the emitted photon is entangled with the spin state [32]. Likewise, a photon absorbed by the NV⁻ center through excitation to this ES may also become entangled with the spin state [33]. Additionally, the coherences between the spin and photons can be probed through the Faraday effect, a nondestructive measurement of the spin state based on shifts of light polarizations [102]. To expand these entanglement protocols to couple one NV⁻ center to another, the emitted photons from each must be indistinguishable. As a solid-state system, each NV⁻ center has slightly different orbital transition energies due to the local electrostatic environment. Tuning the optical transitions of two separate NV⁻ centers to degeneracy can be accomplished through the DC Stark effect with applied external electric fields [84]–[87]. With the ability to tune separate NV⁻ centers to degeneracy [86], interference between an emitted zero-phonon line photon from each NV⁻ center was demonstrated [98], [103] [Fig. 5(c)].

These developments laid the foundation for the demonstration of photonic entanglement of two NV⁻ centers separated by 3 m [35]. In this demonstration, a spin-photon entangled pair was generated for each NV center, and the resulting photons were then overlapped at a beamsplitter and measured jointly in the Bell basis. Successful projection of these time-bin photons in the Bell state heralds the photonic entanglement of the NV centers. Combining the ability to share entanglement over long distances with efforts in developing nuclear spin registries, this was further expanded to unconditionally teleport the nuclear spin state of one NV⁻ center onto the electronic spin state of another distant NV⁻ center [36] [see Fig. 5(e) and (f)]. Tests of fundamental axioms of quantum mechanics have also been demonstrated with NV⁻ centers using a variety of these optical techniques, including the three-quantum box problem [104], as well as the first demonstration of a loophole-free test of Bell's inequality, closing both the locality and detector loopholes [105].

C. Controlling the NV Center With Light

Another route to investigate the NV⁻ center quantum optical interface is to develop methods to actively and fully manipulate the spin with light. As the NV⁻ center acts like a trapped ion in the solid state, a number of atomic physics techniques can be adapted to develop this optical manipulation. Such control occurs within a smaller footprint than previous microwave techniques, down to the spot size of a diffraction-limited laser, which facilitates integration with photonic networks or spin

arrays. One of the earliest demonstrations of optical control in diamond was based on the AC Stark effect that provides a means of rotating the NV⁻ center ground-state spin about the energy eigenbasis axis, creating a phase shift on the qubit state (a Z-axis rotation on the Bloch sphere) [102].

To expand upon this optical control of the NV⁻ center, Λ (lambda) systems can be harnessed [see Fig. 5(d)]. A Λ system consists of two ground states optically coupled to an ES in a level structure resembling its Greek letter namesake [see Fig. 5(d)]. These systems can be optically driven generating control over the GS spin levels. Within this Λ system, coherent population trapping (CPT) is a method to prepare a coherent superposition of the GS, known as the dark state, and has been demonstrated in individual NV⁻ centers [106]–[108] [Fig. 6(a)]. The dark state is a particular superposition of the GS spin sublevels that does not couple to the light fields and as such is determined solely by the relative amplitude and phase of the driving optical fields. Not only does control of a Λ system allow for arbitrary initialization of the GS spin, but also the ability to readout along any arbitrary basis through the transient photoluminescence emitted during CPT, as well as the ability to rotate the spin about any axis via stimulated Raman transitions [109] [Fig. 6(b) and (c)]. By combining these techniques, a full set of single qubit control protocols can be realized and used to measure spin coherence within the NV⁻ center GS. Additionally, control over the dark state superposition can be adiabatically evolved to realize stimulated Raman adiabatic passage (STIRAP) as a method to transfer population from one spin sublevel to another without significant loss through the ES [110]. With the ability to adiabatically evolve dark states within the NV⁻ center, geometric control through optical means has also been realized [78] [Fig. 6(d) and (e)].

Another approach to optically control the GS spin exploits the orbital-light interface in contrast to the spin-light interface. In this case, ultrafast pulses of light are used to transfer spin population between the GS and ES orbitals. The spin dynamics of the excited state can then be probed and used as a method to rotate the spin anywhere on the Bloch sphere. Here, the time spent in the ES dictates the amount of rotation, while the spin mixing of the ES generated by an external magnetic field determines the rotation axis [91] [see Fig. 6(f)]. The ultrafast pulse technique also enables the ability to probe the orbital dynamics through the polarization selectivity of the orbital branches [91].

D. Photonic Structures in Diamond

To further drive the technological application of NV⁻ centers and all-optical control techniques, the development of optically enhancing structures in diamond to couple individual NV⁻ centers has become a growing focus of research. Solid immersion microlenses milled into

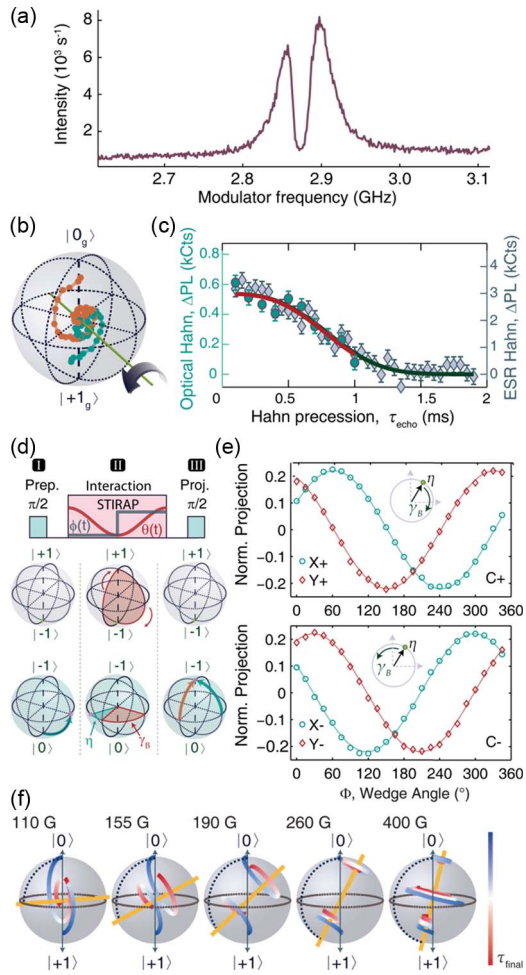


Fig. 6. All-optical control techniques. (a) **Coherent population trapping (CPT) within an NV⁻ center.** Photoluminescence from an NV⁻ center as a function of laser frequency sideband separation. Within a Λ system, when the sideband separation is on resonance with the ground state splitting, the spin is trapped into a dark state, resulting in a dip in PL. Figure from [106]. (b) and (c) **All-optical spin control.** (b) Tomographic reconstruction of spin evolution as a result of stimulated Raman transitions. By detuning from the one-photon resonance within a Λ system, the bright polariton state shifts in energy leading to precession about the bright/dark state axis. (c) A comparison between an all-optical and a microwave approach to measuring transverse spin coherence T_2 . The all-optical approach utilizes Λ system techniques. Figure from [109]. (d) and (e) **Optically accumulated geometric phase.** (d) Pulse sequence to accumulate geometric phase. Placing the spin on the equator of one spin subspace ($0/-1$), and evolving the state through stimulated Raman adiabatic passage on another subspace ($-1/+1$), allows for the ability to measure accumulated geometric phases. (e) Measured projections on ($0/-1$) revealing accumulated geometric phases, proportional to the wedge angle enclosed on the $-1/+1$ Bloch sphere. Figure from [78]. (f) **Spin control derived from excited state dynamics.** Tomographic reconstructions of spin evolution at various different magnetic fields moving through an ES anticrossing. At the center of the anticrossing, the ES spin eigenstates are roughly equal superpositions of 0 and $+1$, leading to an equatorial axis of rotation. Far away from the anticrossing, the eigenstates are largely 0 and $+1$, leading to a largely polar axis of rotation. Figure from [91].

the diamond help improve collection efficiency of the emitted NV⁻ center PL [99], [100], and have enabled a number of advances [19], [35], [36], [91], [95], [105]. Another route to improving the optical interface with the NV⁻ center is through the development of photonic crystals and cavities. As only 3% of the emission of the NV⁻ center is in its zero-phonon line due to strong phonon coupling, these structures aim to increase the zero-phonon line emission and to explore coupling between cavity modes and spin states through Purcell enhancement. Developing photonics is also important for the realization of transferring quantum information via optical networks. While diamond is a challenging material to fabricate, numerous structures have been implemented recently with continuing improvements [111]–[113], including nanowires [114], [115] [Fig. 7(a)], microring resonators [116], photonic crystals [117] [Fig. 7(b)], and nanobeams [118] [Fig. 7(c)].

E. Photonic Structures and Control in SiC

SiC offers an attractive route for photonic development as a more technologically mature material. Available on the wafer scale, and with more developed processing techniques, the potential exists to create cavities with much higher quality factors. Recently, photonic crystals were fabricated in 3C-SiC, with a quality factor $Q \sim 1500$ [Fig. 7(d)] and tuned to the zero phonon line of the Ky5 defect [119]. In addition, photonic crystal nanobeam cavities have shown quality factors as high as 77000 in amorphous SiC [120], and suggest pathways toward high Q photonic crystals in monocrystalline SiC for defect integration. Furthermore, optical control of SiC defects shows promise, as coherent population trapping (CPT) was recently demonstrated in an ensemble of $kh - VV^0$ [121].

V. ELECTRICAL AND MECHANICAL CONTROL OF THE SPIN DEFECT

Another route to controlling spin defects in semiconductors is through the use of electric or strain fields. Such fields address transitions that are magnetic-dipole forbidden, those between spin sublevels of $\Delta m_s = 2$. These spin sublevels are coupled to the electric field due to the Stark effect, a result of both spin–spin and spin–orbit interactions. Due to the symmetry of these defects, electric and strain fields act in a similar manner. This coupling to electric fields was first seen in ensembles of NV⁻ centers as a shift in the GS spin transitions through a modulation of a spin echo [122]. Since then, there have been a variety of control and sensing applications exploiting this electrical and mechanical interface.

A. Mechanical Control in Defect Spins

Strain, often mediated by mechanical motion, is the basis for a series of novel control techniques applied to

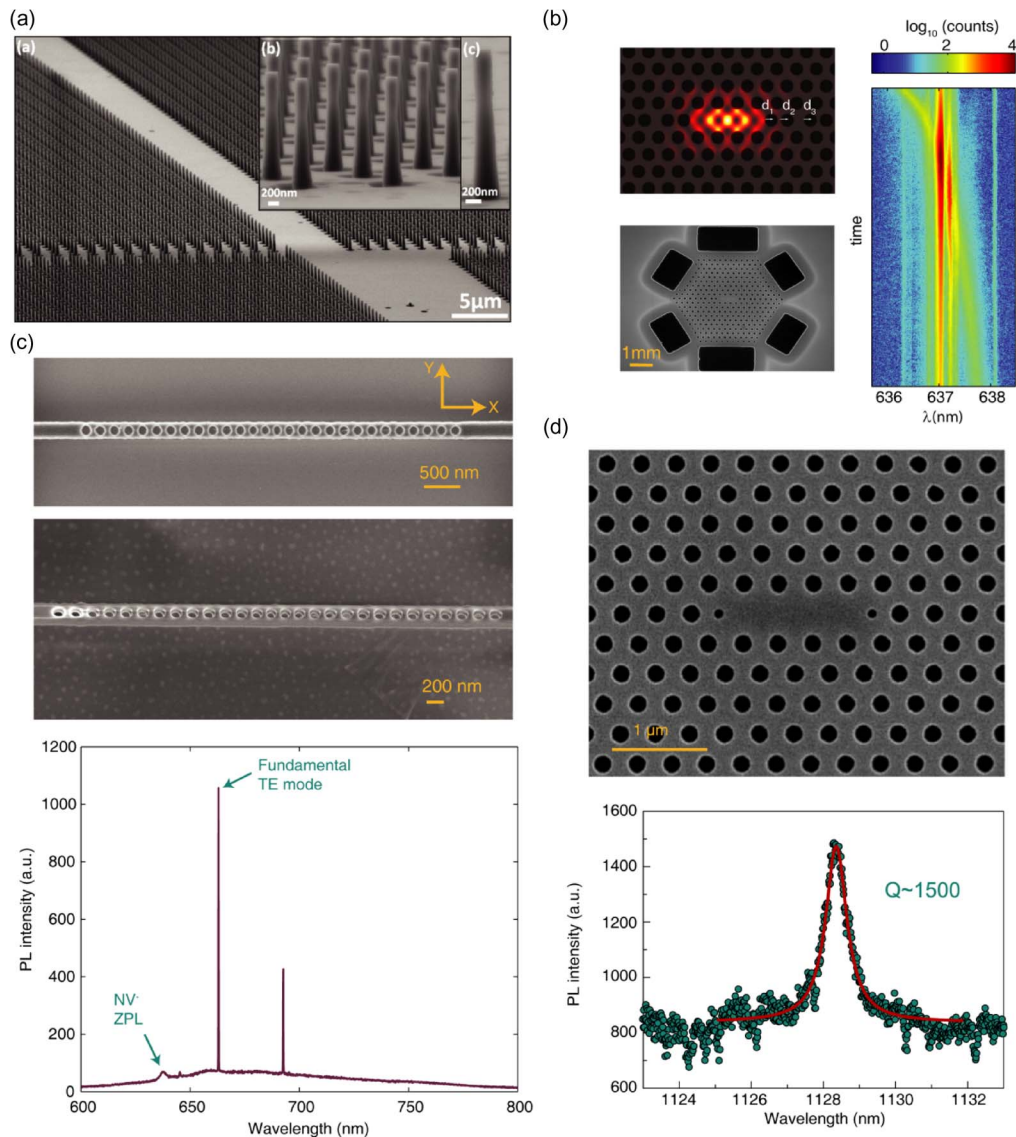


Fig. 7. Photonic structures in diamond and SiC. (a) An array of nanowires $\sim 2 \mu\text{m}$ in height, $\sim 200 \text{ nm}$ in diameter in diamond imaged via SEM. The array was realized via high-throughput nanofabrication techniques and $>10\%$ of the devices contain a single NV^- center. NV^- centers have been realized in nanowires through a variety of techniques including prefabrication and postfabrication implantation and annealing, as well as through delta doping and irradiation. Figure from [114]. (b) Photonic crystal in diamond. Top left: A three-hole defect shifted cavity and the electric-field energy density of its fundamental mode. The three holes are shifted by d_1 , d_2 , and d_3 . Bottom left: SEM image of three-hole defect cavity. Right: Color plot of photoluminescence measured by tuning the cavity resonance across the ZPL of the NV^- center ensemble. Figure from [117]. (c) Nanobeam photonic cavity fabricated in diamond. Nanobeams have become one of the preferred methods in diamond due to their low mode volume and the ability to achieve modest quality factors ~ 10000 . Top: SEM image of a nanobeam containing delta-doped NV^- centers. Bottom: The fundamental mode of the nanobeam in relation to the NV^- center spectra. The cavity resonance can be altered through gas tuning. Figure from [118]. (d) Photonic crystal in SiC. Top, SEM image of an L3 photonic crystal in SiC. Bottom: Enhancement of the ZPL of the Ky5 center in SiC reveals a $Q \sim 1500$. Figure from [119].

defect spins. By applying stress waves through a MEMS transducer on a diamond, magnetic-dipole forbidden transitions within the NV^- center ground state can be driven, and optically detected mechanical spin resonance for an ensemble of NV^- centers can be observed [123] [Fig. 8(a)]. This technique can further be extended to

drive Rabi oscillations between the $\Delta m_s = 2$ transitions [124] [Fig. 8(b)]. Additionally, a diamond cantilever driven by a time-varying strain field can induce Rabi oscillations within a single NV^- center [125]. Likewise, because of this coupling, examining a series of NV^- centers within a strained cantilever reveals a sensitive map

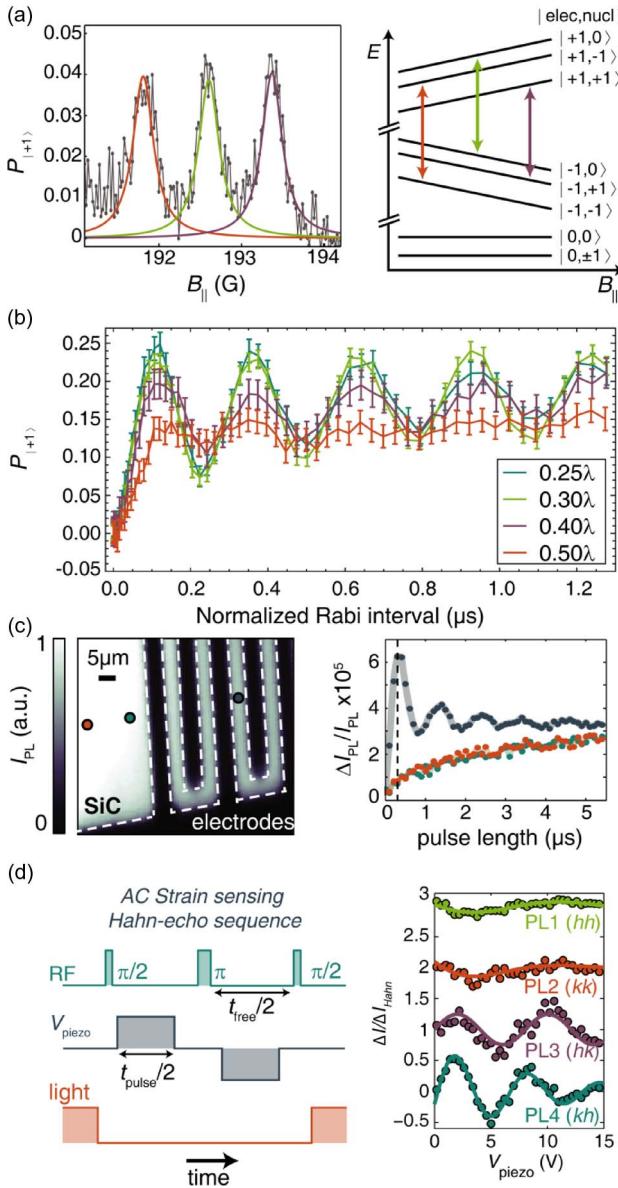


Fig. 8. Mechanical and electrical control of spin defects. (a) *Optically detected mechanical spin resonance. Left: For a fixed driving frequency of 1.076 GHz, the population that is driven into the $m_s = +1$ from $m_s = -1$ as a function of magnetic field. Right: NV^- center hyperfine levels with each arrow corresponding to the condition that the transition indicated is in resonance with the mechanical drive. Figure from [123].* (b) *Mechanically-driven Rabi oscillations of NV^- center ensembles at different depths within the sample, where λ corresponds to the wavelength of the standing stress wave. Figure from [124].* (c) *Electrically-driven Rabi oscillations of VV^0 ensembles in 6H-SiC. Left: PL from sample indicating the electrodes. Right: electrically-driven Rabi oscillations for the three regions denoted by the colored circles indicating the oscillations are confined to within the electrodes. Figure from [129].* (d) *AC strain sensing with VV^0 ensembles in 4H-SiC. Left: Hahn-echo pulse sequence for strain sensing. Right: The strain phase shifts the spin superposition during the free evolution portions, and has significantly different effects on the different divacancy configurations. Figure from [44].*

of both the axial and transverse strains [126]. Alternatively, mechanical motion has been coupled to the NV^- center spin by driving a resonator coated with a magnetic film, leading to an oscillating magnetic field driving the magnetic-dipole transitions [127], [128] ($\Delta m_s = 1$) as opposed to those driving the dipole-forbidden transitions. These demonstrations reveal a diversity of approaches to coupling mechanical degrees of freedom to spin degrees of freedom within optically addressable defects, and as such they suggest routes toward optomechanical transducers.

B. Electrical Control in Defect Spins

Electric fields are typically used to tune the orbital levels of the excited state through the DC Stark effect [35], [84]–[87], [98], [103] for photonic applications. However, they also couple, albeit more weakly, to the ground state spin sublevels ($\Delta m_s = 2$), and control of these levels has been seen not only in NV^- centers but also in the VV^0 in SiC. In particular, the E-field coupling term has allowed for the ability to sense electric fields at the nanoscale within NV^- centers [3]. In SiC, electrically-driven spin resonance has been demonstrated in ensembles of VV^0 centers, and extended to drive Rabi oscillations between $m_s = \pm 1$ states ($\Delta m_s = 2$) [129] [Fig. 8(c)]. Such control is limited to between lithographically deposited electrodes on the sample, suggesting good confinement of the control field. In addition, the ability to sense these electric fields in SiC reveals an electric dipole moment that is roughly twice as large as the NV^- center, and provides an alternative system in which to sense nanoscale electric and strain fields [44] [Fig. 8(d)].

VI. DISCUSSION AND CONCLUSION

Spin defects in semiconductors have come a long way in the past few decades. While their ultimate aim as a solid-state qubit for quantum logic may still be years away, other elements of a quantum network, such as quantum repeaters, may be realized much sooner. With the recent achievement of state teleportation between two distant NV^- centers [36] and improvements in photonic devices [113], building up to a multinode quantum network may be possible with further technical improvements [83]. These spin defects could ultimately find their niche as nanoscale sensors, providing high-resolution spatial metrology of electric and magnetic fields, and temperature [66]. As diamond is biocompatible with low toxicity, nanoparticles could also be used within living systems [41], [69], [70].

All these applications are facilitated by the wide range of quantum control mechanisms available. Microwave control enables the ability to dynamically decouple these spin defects from their environment, while photonic control may aid in the integration with photonic

structures and the development of quantum photonic networks. Alternatively, electric and mechanical control of spin defects could open up different degrees of freedom and provide a means to couple these defects to other quantum systems. Together, this versatility could lead to the development of quantum hybrid systems,

leveraging the strengths of disparate systems. Further material studies of spin defects in wide-bandgap materials may also yield new spin defects in host materials that allow for even greater quantum control. The future is bright for these optically addressable defects, and they will continue to drive quantum technologies forward. ■

REFERENCES

- [1] D. P. DiVincenzo, "The physical implementation of quantum computation," *Fortschritte der Phys.*, vol. 48, no. 9–11, pp. 771–783, Sep. 2000.
- [2] J. M. Taylor *et al.*, "High-sensitivity diamond magnetometer with nanoscale resolution," *Nature Phys.*, vol. 4, no. 10, pp. 810–816, Oct. 2008.
- [3] F. Dolde *et al.*, "Electric-field sensing using single diamond spins," *Nature Phys.*, vol. 7, no. 6, pp. 459–463, Jun. 2011.
- [4] D. M. Toyli *et al.*, "Measurement and control of single nitrogen-vacancy center spins above 600 K," *Phys. Rev. X*, vol. 2, no. 3, Jul. 2012, Art. no. 031001.
- [5] M. A. Nielsen and I. Chuang, *Quantum Computation and Quantum Information*. Cambridge, U.K.: Cambridge Univ. Press, 2000.
- [6] G. D. Fuchs, G. Burkard, P. V. Klimov, and D. D. Awschalom, "A quantum memory intrinsic to single nitrogen–Vacancy centres in diamond," *Nature Phys.*, vol. 7, no. 10, pp. 789–793, Oct. 2011.
- [7] M. V. Gurudev Dutt *et al.*, "Quantum register based on individual electronic and nuclear spin qubits in diamond," *Science*, vol. 316, no. 5829, pp. 1312–1316, Jun. 2007.
- [8] P. C. Maurer *et al.*, "Room-temperature quantum bit memory exceeding one second," *Science*, vol. 336, no. 6086, pp. 1283–1286, Jun. 2012.
- [9] W. Pfaff *et al.*, "Demonstration of entanglement-by-measurement of solid-state qubits," *Nature Phys.*, vol. 9, no. 1, pp. 29–33, Jan. 2013.
- [10] T. H. Taminiau, J. Cramer, T. van der Sar, V. V. Dobrovitski, and R. Hanson, "Universal control and error correction in multi-qubit spin registers in diamond," *Nature Nanotechnol.*, vol. 9, no. 3, pp. 171–176, Mar. 2014.
- [11] P. V. Klimov, A. L. Falk, D. J. Christle, V. V. Dobrovitski, and D. D. Awschalom, "Quantum entanglement at ambient conditions in a macroscopic solid-state spin ensemble," *Sci. Adv.*, vol. 1, no. 10, Nov. 2015, Art. no. e1501015.
- [12] G. Davies and M. F. Hamer, "Optical studies of the 1.945 eV vibronic band in diamond," *Proc. R. Soc. Lond. A, Math. Phys. Sci.*, vol. 348, no. 1653, pp. 285–298, Feb. 1976.
- [13] A. Gruber *et al.*, "Scanning confocal optical microscopy and magnetic resonance on single defect centers," *Science*, vol. 276, no. 5321, pp. 2012–2014, Jun. 1997.
- [14] M. W. Doherty *et al.*, "The nitrogen-vacancy colour centre in diamond," *Phys. Rep.*, vol. 528, no. 1, pp. 1–45, Jul. 2013.
- [15] C. Hepp *et al.*, "Electronic structure of the silicon vacancy color center in diamond," *Phys. Rev. Lett.*, vol. 112, no. 3, Jan. 2014, Art. no. 036405.
- [16] T. Müller *et al.*, "Optical signatures of silicon-vacancy spins in diamond," *Nature Commun.*, vol. 5, Feb. 2014, Art. no. 3328.
- [17] A. Sipahigil *et al.*, "Indistinguishable photons from separated silicon-vacancy centers in diamond," *Phys. Rev. Lett.*, vol. 113, no. 11, Sep. 2014, Art. no. 113602.
- [18] P. G. Baranov *et al.*, "Silicon vacancy in SiC as a promising quantum system for single-defect and single-photon spectroscopy," *Phys. Rev. B*, vol. 83, no. 12, Mar. 2011, Art. no. 125203.
- [19] M. Widmann *et al.*, "Coherent control of single spins in silicon carbide at room temperature," *Nature Mater.*, vol. 14, no. 2, pp. 164–168, Feb. 2015.
- [20] N. T. Son *et al.*, "Divacancy in 4H-SiC," *Phys. Rev. Lett.*, vol. 96, no. 5, Feb. 2006, Art. no. 055501.
- [21] W. F. Koehl, B. B. Buckley, F. J. Heremans, G. Calusine, and D. D. Awschalom, "Room temperature coherent control of defect spin qubits in silicon carbide," *Nature*, vol. 479, no. 7371, pp. 84–87, Nov. 2011.
- [22] A. L. Falk *et al.*, "Polytype control of spin qubits in silicon carbide," *Nature Commun.*, vol. 4, May 2013, Art. no. 1819.
- [23] D. J. Christle *et al.*, "Isolated electron spins in silicon carbide with millisecond coherence times," *Nature Mater.*, vol. 14, no. 2, pp. 160–163, Feb. 2015.
- [24] S. Castelletto *et al.*, "A silicon carbide room-temperature single-photon source," *Nature Mater.*, vol. 13, no. 2, pp. 151–156, Feb. 2014.
- [25] N. R. Jungwirth *et al.*, "A single-molecule approach to ZnO defect studies: Single photons and single defects," *J. Appl. Phys.*, vol. 116, no. 4, Jul. 2014, Art. no. 043509.
- [26] J. R. Weber *et al.*, "Quantum computing with defects," *Proc. Nat. Acad. Sci. USA*, vol. 107, no. 19, pp. 8513–8518, May 2010.
- [27] J. H. N. Loubser and J. A. van Wyk, "Optical spin-polarisation in a triplet state in irradiated and annealed Type Ib diamond," *Diamond Res.*, vol. 9, pp. 11–14, 1977.
- [28] J. H. N. Loubser and J. A. van Wyk, "Electron spin resonance in the study of diamond," *Rep. Progr. Phys.*, vol. 41, pp. 1201–1245, 1978.
- [29] L. Du Preez, "Electron paramagnetic resonance and optical investigations of defect centres in diamond," Univ. Witwatersrand, Johannesburg, South Africa, 1965.
- [30] G. Balasubramanian *et al.*, "Ultralong spin coherence time in isotopically engineered diamond," *Nature Mater.*, vol. 8, no. 5, pp. 383–387, May 2009.
- [31] L. Childress, J. M. Taylor, A. S. Sorenson, and M. D. Lukin, "Fault-tolerant quantum repeaters with minimal physical resources and implementations based on single-photon emitters," *Phys. Rev. A*, vol. 72, no. 5, Nov. 2005, Art. no. 052330.
- [32] E. Togan *et al.*, "Quantum entanglement between an optical photon and a solid-state spin qubit," *Nature*, vol. 466, no. 7307, pp. 730–734, Aug. 2010.
- [33] H. Kosaka and N. Niikura, "Entangled absorption of a single photon with a single spin in diamond," *Phys. Rev. Lett.*, vol. 114, no. 5, Feb. 2015, Art. no. 53603.
- [34] F. Dolde *et al.*, "Room-temperature entanglement between single defect spins in diamond," *Nature Phys.*, vol. 9, no. 3, pp. 139–143, Mar. 2013.
- [35] H. Bernien *et al.*, "Heralded entanglement between solid-state qubits separated by three metres," *Nature*, vol. 497, no. 7447, pp. 86–90, May 2013.
- [36] W. Pfaff *et al.*, "Unconditional quantum teleportation between distant solid-state quantum bits," *Science*, vol. 345, no. 6196, pp. 532–535, Aug. 2014.
- [37] G. Balasubramanian *et al.*, "Nanoscale imaging magnetometry with diamond spins under ambient conditions," *Nature*, vol. 455, no. 7213, pp. 648–651, Oct. 2008.
- [38] J. R. Maze *et al.*, "Nanoscale magnetic sensing with an individual electronic spin in diamond," *Nature*, vol. 455, no. 7213, pp. 644–647, Oct. 2008.
- [39] D. M. Toyli, C. F. de las Casas, D. J. Christle, V. V. Dobrovitski, and D. D. Awschalom, "Fluorescence thermometry enhanced by the quantum coherence of single spins in diamond," *Proc. Nat. Acad. Sci. USA*, vol. 110, no. 21, pp. 8417–8421, May 2013.
- [40] P. Neumann *et al.*, "High-precision nanoscale temperature sensing using single defects in diamond," *Nano Lett.*, vol. 13, no. 6, pp. 2738–2742, Jun. 2013.
- [41] G. Kucsko *et al.*, "Nanometre-scale thermometry in a living cell," *Nature*, vol. 500, no. 7460, pp. 54–58, Aug. 2013.
- [42] P. G. Baranov *et al.*, "EPR identification of the triplet ground state and photoinduced population inversion for a Si-C divacancy in silicon carbide," *J. Exp. Theor. Phys. Lett.*, vol. 82, no. 7, pp. 441–443, Oct. 2005.
- [43] Á. Gali, "Time-dependent density functional study on the excitation spectrum of point defects in semiconductors," *Phys. Status Solidi B*, vol. 248, no. 6, pp. 1337–1346, Jun. 2011.
- [44] A. L. Falk *et al.*, "Electrically and mechanically tunable electron spins in silicon carbide color centers," *Phys. Rev. Lett.*, vol. 112, no. 18, May 2014, Art. no. 187601.
- [45] L. Childress *et al.*, "Coherent dynamics of coupled electron and nuclear spin qubits in diamond," *Science*, vol. 314, no. 5797, pp. 281–285, Oct. 2006.
- [46] L.-P. Yang *et al.*, "Electron spin decoherence in silicon carbide nuclear spin bath," *Phys. Rev. B*, vol. 90, no. 24, Dec. 2014, Art. no. 241203.
- [47] S. G. Carter, Ö. O. Soykal, P. Dev, S. E. Economou, and E. R. Glaser, "Spin coherence and echo modulation of the silicon vacancy in 4H-SiC at room temperature," *Phys. Rev. B*, vol. 92, no. 16, Oct. 2015, Art. no. 161202(R).
- [48] A. Jarmola, V. M. Acosta, K. Jensen, S. Chemerisov, and D. Budker, "Temperature- and magnetic-field-dependent

- longitudinal spin relaxation in nitrogen-vacancy ensembles in diamond," *Phys. Rev. Lett.*, vol. 108, no. 19, May 2012, Art. no. 197601.
- [49] P. Siyushev *et al.*, "Optically controlled switching of the charge state of a single nitrogen-vacancy center in diamond at cryogenic temperatures," *Phys. Rev. Lett.*, vol. 110, no. 16, Apr. 2013, Art. no. 167402.
- [50] T. Plakhotnik, H. Aman, and H.-C. Chang, "All-optical single-nanoparticle ratiometric thermometry with a noise floor of $0.3 \text{ K Hz}^{-1/2}$," *Nanotechnology*, vol. 26, no. 24, May 2015, Art. no. 245501.
- [51] K. Ohno *et al.*, "Engineering shallow spins in diamond with nitrogen delta-doping," *Appl. Phys. Lett.*, vol. 101, no. 8, 2012, Art. no. 082413.
- [52] I. I. Rabi, "Space quantization in a gyrating magnetic field," *Phys. Rev.*, vol. 51, no. 8, Apr. 1937, Art. no. 652.
- [53] F. Jelezko, T. Gaebel, I. Popa, A. Gruber, and J. Wrachtrup, "Observation of coherent oscillations in a single electron spin," *Phys. Rev. Lett.*, vol. 92, no. 7, Feb. 2004, Art. no. 076401.
- [54] G. D. Fuchs, V. V. Dobrovitski, D. M. Toyli, F. J. Heremans, and D. D. Awschalom, "Gigahertz dynamics of a strongly driven single quantum spin," *Science*, vol. 326, no. 5959, pp. 1520–1522, Dec. 2009.
- [55] G. D. Fuchs *et al.*, "Excited-state spin coherence of a single nitrogen-vacancy centre in diamond," *Nature Phys.*, vol. 6, no. 9, pp. 668–672, Sep. 2010.
- [56] N. F. Ramsey, "A molecular beam resonance method with separated oscillating fields," *Phys. Rev.*, vol. 78, no. 6, pp. 695–699, Jun. 1950.
- [57] E. Hahn, "Spin Echoes," *Phys. Rev.*, vol. 80, no. 4, pp. 580–594, Nov. 1950.
- [58] G. de Lange, Z. H. Wang, D. Ristè, V. V. Dobrovitski, and R. Hanson, "Universal dynamical decoupling of a single solid-state spin from a spin bath," *Science*, vol. 330, no. 6000, pp. 60–63, Oct. 2010.
- [59] C. A. Ryan, J. S. Hodges, and D. G. Cory, "Robust decoupling techniques to extend quantum coherence in diamond," *Phys. Rev. Lett.*, vol. 105, no. 20, Nov. 2010, Art. no. 200402.
- [60] N. Bar-Gill, L. M. Pham, A. Jarmola, D. Budker, and R. L. Walsworth, "Solid-state electronic spin coherence time approaching one second," *Nature Commun.*, vol. 4, Apr. 2013, Art. no. 1743.
- [61] T. van der Sar *et al.*, "Decoherence-protected quantum gates for a hybrid solid-state spin register," *Nature*, vol. 484, no. 7392, pp. 82–86, Apr. 2012.
- [62] T. Ishikawa *et al.*, "Optical and spin coherence properties of nitrogen-vacancy centers placed in a 100 nm thick isotopically purified diamond layer," *Nano Lett.*, vol. 12, no. 4, pp. 2083–2087, Apr. 2012.
- [63] S. Steinert *et al.*, "High sensitivity magnetic imaging using an array of spins in diamond," *Rev. Sci. Instrum.*, vol. 81, no. 4, Apr. 2010, Art. no. 043705.
- [64] B. J. Maertz, A. P. Wijnheijmer, G. D. Fuchs, M. E. Nowakowski, and D. D. Awschalom, "Vector magnetic field microscopy using nitrogen vacancy centers in diamond," *Appl. Phys. Lett.*, vol. 96, no. 9, Mar. 2010, Art. no. 092504.
- [65] G. de Lange, D. Ristè, V. V. Dobrovitski, and R. Hanson, "Single-spin magnetometry with multipulse sensing sequences," *Phys. Rev. Lett.*, vol. 106, no. 8, Feb. 2011, Art. no. 080802.
- [66] L. Rondin *et al.*, "Magnetometry with nitrogen-vacancy defects in diamond," *Reports Prog. Phys.*, vol. 77, no. 5, May 2014, Art. no. 056503.
- [67] H. J. Mamin *et al.*, "Nanoscale nuclear magnetic resonance with a nitrogen-vacancy spin sensor," *Science*, vol. 339, no. 6119, pp. 557–560, Feb. 2013.
- [68] T. Staudacher *et al.*, "Nuclear magnetic resonance spectroscopy on a (5-nanometer)³ sample volume," *Science*, vol. 339, no. 6119, pp. 561–563, Feb. 2013.
- [69] L. P. McGuinness *et al.*, "Quantum measurement and orientation tracking of fluorescent nanodiamonds inside living cells," *Nature Nanotechnol.*, vol. 6, no. 6, pp. 358–363, Jun. 2011.
- [70] D. Le Sage *et al.*, "Optical magnetic imaging of living cells," *Nature*, vol. 496, no. 7446, pp. 486–489, Apr. 2013.
- [71] D. Rugar *et al.*, "Proton magnetic resonance imaging using a nitrogen-vacancy spin sensor," *Nature Nanotechnol.*, vol. 10, no. 2, pp. 120–124, Feb. 2014.
- [72] S. Steinert *et al.*, "Magnetic spin imaging under ambient conditions with sub-cellular resolution," *Nature Commun.*, vol. 4, Mar. 2013, Art. no. 1607.
- [73] A. O. Sushkov *et al.*, "All-optical sensing of a single-molecule electron spin," *Nano Lett.*, vol. 14, no. 11, pp. 6443–6448, Nov. 2014.
- [74] L. T. Hall *et al.*, "Detection of nanoscale electron spin resonance spectra demonstrated using nitrogen-vacancy centre probes in diamond," *Nature Commun.*, vol. 7, Jan. 2016, Art. no. 10211.
- [75] V. M. Acosta *et al.*, "Temperature dependence of the nitrogen-vacancy magnetic resonance in diamond," *Phys. Rev. Lett.*, vol. 104, no. 7, Feb. 2010, Art. no. 070801.
- [76] M. W. Doherty *et al.*, "Temperature shifts of the resonances of the NV-center in diamond," *Phys. Rev. B*, vol. 90, no. 4, Jul. 2014, Art. no. 041201(R).
- [77] K. Zhang, N. M. Nusran, B. R. Slezak, and M. V. Gurudev Dutt, "Measurement of the Berry phase in a single solid-state spin qubit," 2014. [Online]. Available: <http://arxiv.org/abs/1410.2791>
- [78] C. G. Yale *et al.*, "Optical manipulation of the Berry phase in a solid-state spin qubit," *Nature Photon.*, vol. 10, no. 3, pp. 184–189, Mar. 2016.
- [79] C. Zu *et al.*, "Experimental realization of universal geometric quantum gates with solid-state spins," *Nature*, vol. 514, no. 7520, pp. 72–75, Oct. 2014.
- [80] S. Arroyo-Camejo, A. Lazariev, S. W. Hell, and G. Balasubramanian, "Room temperature high-fidelity holonomic single-qubit gate on a solid-state spin," *Nature Commun.*, vol. 5, Sep. 2014, Art. no. 4870.
- [81] S. Berger *et al.*, "Exploring the effect of noise on the Berry phase," *Phys. Rev. A*, vol. 87, no. 6, Jun. 2013, Art. no. 060303(R).
- [82] G. De Chiara and G. M. Palma, "Berry phase for a spin 1/2 particle in a classical fluctuating field," *Phys. Rev. Lett.*, vol. 91, no. 9, Aug. 2003, Art. no. 090404.
- [83] W. B. Gao, A. Imamoglu, H. Bernien, and R. Hanson, "Coherent manipulation, measurement and entanglement of individual solid-state spins using optical fields," *Nature Photon.*, vol. 9, no. 6, pp. 363–373, Jun. 2015.
- [84] P. Tamarat *et al.*, "Stark shift control of single optical centers in diamond," *Phys. Rev. Lett.*, vol. 97, no. 8, Aug. 2006, Art. no. 083002.
- [85] P. Tamarat *et al.*, "Spin-flip and spin-conserving optical transitions of the nitrogen-vacancy centre in diamond," *New J. Phys.*, vol. 10, Apr. 2008, Art. no. 045004.
- [86] L. C. Bassett, F. J. Heremans, C. G. Yale, B. B. Buckley, and D. D. Awschalom, "Electrical tuning of single nitrogen-vacancy center optical transitions enhanced by photoinduced fields," *Phys. Rev. Lett.*, vol. 107, no. 26, Dec. 2011, Art. no. 266403.
- [87] V. M. Acosta *et al.*, "Dynamic stabilization of the optical resonances of single nitrogen-vacancy centers in diamond," *Phys. Rev. Lett.*, vol. 108, no. 20, May 2012, Art. no. 206401.
- [88] M. W. Doherty, N. B. Manson, P. Delaney, and L. C. L. Hollenberg, "The negatively charged nitrogen-vacancy centre in diamond: The electronic solution," *New J. Phys.*, vol. 13, Feb. 2011, Art. no. 025019.
- [89] J. R. Maze *et al.*, "Properties of nitrogen-vacancy centers in diamond: The group theoretic approach," *New J. Phys.*, vol. 13, Feb. 2011, Art. no. 025025.
- [90] A. Batalov *et al.*, "Low temperature studies of the excited-state structure of negatively charged nitrogen-vacancy color centers in diamond," *Phys. Rev. Lett.*, vol. 102, no. 19, May 2009, Art. no. 195506.
- [91] L. C. Bassett *et al.*, "Ultrafast optical control of orbital and spin dynamics in a solid-state defect," *Science*, vol. 345, no. 6202, pp. 1333–1337, Sep. 2014.
- [92] K. M. Fu *et al.*, "Observation of the dynamic Jahn-Teller effect in the excited states of nitrogen-vacancy centers in diamond," *Phys. Rev. Lett.*, vol. 103, no. 25, Dec. 2009, Art. no. 256404.
- [93] L. J. Rogers, R. L. McMurtrie, M. J. Sellars, and N. B. Manson, "Time-averaging within the excited state of the nitrogen-vacancy centre in diamond," *New J. Phys.*, vol. 11, no. 6, Jun. 2009, Art. no. 063007.
- [94] F. Jelezko *et al.*, "Single spin states in a defect center resolved by optical spectroscopy," *Appl. Phys. Lett.*, vol. 81, no. 2002, pp. 2160–2162, Sep. 2002.
- [95] L. Robledo *et al.*, "High-fidelity projective read-out of a solid-state spin quantum register," *Nature*, vol. 477, no. 7366, pp. 574–578, Sep. 2011.
- [96] H. B. Dyer, F. A. Raal, L. Du Preez, and J. H. N. Loubser, "Optical absorption features associated with paramagnetic nitrogen in diamond," *Philosoph. Mag.*, vol. 11, no. 112, pp. 763–774, Apr. 1965.
- [97] F. J. Heremans, G. D. Fuchs, C. F. Wang, R. Hanson, and D. D. Awschalom, "Generation and transport of photoexcited electrons in single-crystal diamond," *Appl. Phys. Lett.*, vol. 94, no. 15, Apr. 2009, Art. no. 152102.
- [98] H. Bernien *et al.*, "Two-photon quantum interference from separate nitrogen vacancy centers in diamond," *Phys. Rev. Lett.*, vol. 108, no. 4, Jan. 2012, Art. no. 043604.
- [99] P. Siyushev *et al.*, "Monolithic diamond optics for single photon detection," *Appl. Phys. Lett.*, vol. 97, no. 24, Dec. 2010, Art. no. 241902.
- [100] J. P. Hadden *et al.*, "Strongly enhanced photon collection from diamond defect

- centers under microfabricated integrated solid immersion lenses," *Appl. Phys. Lett.*, vol. 97, no. 24, Dec. 2010, Art. no. 241901.
- [101] L. Robledo, H. Bernien, I. van Weperen, and R. Hanson, "Control and coherence of the optical transition of single nitrogen vacancy centers in diamond," *Phys. Rev. Lett.*, vol. 105, no. 17, Oct. 2010, Art. no. 177403.
- [102] B. B. Buckley, G. D. Fuchs, L. C. Bassett, and D. D. Awschalom, "Spin-light coherence for single-spin measurement and control in diamond," *Science*, vol. 330, no. 6008, pp. 1212–1215, Nov. 2010.
- [103] A. Sipahigil *et al.*, "Quantum interference of single photons from remote nitrogen-vacancy centers in diamond," *Phys. Rev. Lett.*, vol. 108, no. 14, Apr. 2012, Art. no. 143601.
- [104] R. E. George *et al.*, "Opening up three quantum boxes causes classically undetectable wavefunction collapse," *Proc. Nat. Acad. Sci. USA*, vol. 110, no. 10, pp. 3777–3781, Mar. 2013.
- [105] B. Hensen *et al.*, "Loophole-free Bell inequality violation using electron spins separated by 1.3 kilometres," *Nature*, vol. 526, no. 7575, pp. 682–686, Oct. 2015.
- [106] C. Santori *et al.*, "Coherent population trapping of single spins in diamond under optical excitation," *Phys. Rev. Lett.*, vol. 97, no. 24, Dec. 2006, Art. no. 247401.
- [107] E. Togan, Y. Chu, A. Imamoglu, and M. D. Lukin, "Laser cooling and real-time measurement of the nuclear spin environment of a solid-state qubit," *Nature*, vol. 478, no. 7370, pp. 497–501, Oct. 2011.
- [108] D. A. Golter, K. N. Dinyari, and H. Wang, "Nuclear-spin-dependent coherent population trapping of single nitrogen-vacancy centers in diamond," *Phys. Rev. A*, vol. 87, no. 3, Mar. 2013, Art. no. 035801.
- [109] C. G. Yale *et al.*, "All-optical control of a solid-state spin using coherent dark states," *Proc. Nat. Acad. Sci. USA*, vol. 110, no. 19, pp. 7595–7600, May 2013.
- [110] D. A. Golter and H. Wang, "Optically driven rabi oscillations and adiabatic passage of single electron spins in diamond," *Phys. Rev. Lett.*, vol. 112, no. 11, Mar. 2014, Art. no. 116403.
- [111] I. Aharonovich, A. D. Greentree, and S. Praver, "Diamond photonics," *Nature Photon.*, vol. 5, no. 7, pp. 397–405, Jul. 2011.
- [112] M. Lončar and A. Faraon, "Quantum photonic networks in diamond," *MRS Bull.*, vol. 38, no. 2, pp. 144–148, Feb. 2013.
- [113] T. Schröder *et al.*, "Quantum nanophotonics in diamond," *J. Opt. Soc. Amer. B*, vol. 33, no. 4, pp. B65–B83, Apr. 2016.
- [114] B. J. M. Hausmann *et al.*, "Single-color centers implanted in diamond nanostructures," *New J. Phys.*, vol. 13, no. 4, Apr. 2011, Art. no. 045004.
- [115] T. M. Babinec *et al.*, "A diamond nanowire single-photon source," *Nature Nanotechnol.*, vol. 5, no. 3, pp. 195–199, Mar. 2010.
- [116] A. Faraon, P. E. Barclay, C. Santori, K. M. C. Fu, and R. G. Beausoleil, "Resonant enhancement of the zero-phonon emission from a colour centre in a diamond cavity," *Nature Photon.*, vol. 5, no. 5, pp. 301–305, May 2011.
- [117] A. Faraon, C. Santori, Z. H. Huang, V. M. Acosta, and R. G. Beausoleil, "Coupling of nitrogen-vacancy centers to photonic crystal cavities in monocrystalline diamond," *Phys. Rev. Lett.*, vol. 109, no. 3, Jul. 2012, Art. no. 033604.
- [118] J. C. Lee *et al.*, "Deterministic coupling of delta-doped nitrogen vacancy centers to a nanobeam photonic crystal cavity," *Appl. Phys. Lett.*, vol. 105, no. 26, Dec. 2014, Art. no. 261101.
- [119] G. Calusine, A. Politi, and D. D. Awschalom, "Silicon carbide photonic crystal cavities with integrated color centers," *Appl. Phys. Lett.*, vol. 105, no. 1, Jul. 2014, Art. no. 011123.
- [120] J. Y. Lee, X. Lu, and Q. Lin, "High-Q silicon carbide photonic-crystal cavities," *Appl. Phys. Lett.*, vol. 106, no. 4, Jan. 2015, Art. no. 041106.
- [121] O. V. Zwiher, D. O'Shea, A. R. Onur, and C. H. van der Wal, "All-optical coherent population trapping with defect spin ensembles in silicon carbide," *Sci. Rep.*, vol. 5, Jan. 2015, Art. no. 10931.
- [122] E. Van Oort and M. Glasbeek, "Electric-field-induced modulation of spin echoes of N-V centers in diamond," *Chem. Phys. Lett.*, vol. 168, no. 6, pp. 529–532, May 1990.
- [123] E. R. MacQuarrie, T. A. Gosavi, N. R. Jungwirth, S. A. Bhawe, and G. D. Fuchs, "Mechanical spin control of nitrogen-vacancy centers in diamond," *Phys. Rev. Lett.*, vol. 111, no. 22, Nov. 2013, Art. no. 227602.
- [124] E. R. MacQuarrie *et al.*, "Coherent control of a nitrogen-vacancy center spin ensemble with a diamond mechanical resonator," *Optica*, vol. 2, no. 3, pp. 233–238, Mar. 2015.
- [125] A. Barfuss, J. Teissier, E. Neu, A. Nunnenkamp, and P. Maletinsky, "Strong mechanical driving of a single electron spin," *Nature Phys.*, vol. 11, no. 10, pp. 820–824, Oct. 2015.
- [126] P. Ovartchaiyapong, K. W. Lee, B. A. Myers, and A. C. Bleszynski Jayich, "Dynamic strain-mediated coupling of a single diamond spin to a mechanical resonator," *Nature Commun.*, vol. 5, Jan. 2014, Art. no. 4429.
- [127] S. K. Hong *et al.*, "Coherent, mechanical control of a single electronic spin," *Nano Lett.*, vol. 12, no. 8, pp. 3920–3924, Aug. 2012.
- [128] S. Kolkowitz *et al.*, "Coherent sensing of a mechanical resonator with a single-spin qubit," *Science*, vol. 335, no. 6076, pp. 1603–1606, Mar. 2012.
- [129] P. V. Klimov, A. L. Falk, B. B. Buckley, and D. D. Awschalom, "Electrically driven spin resonance in silicon carbide color centers," *Phys. Rev. Lett.*, vol. 112, no. 8, Feb. 2013, Art. no. 087601.

ABOUT THE AUTHORS

F. Joseph Heremans (Member, IEEE) received the B.S.E. degree in computer engineering and the B.M. degree in music theory from the University of Michigan, Ann Arbor, MI, USA, in 2006 and the Ph.D. degree in electrical engineering from the University of California Santa Barbara, Santa Barbara, CA, USA, in 2013.

He is currently a Staff Scientist in the Quantum Metamaterials Lab, Argonne National Laboratory, Argonne, IL, USA and a visiting Scientist at the Institute for Molecular Engineering, University of Chicago, Chicago, IL, USA. His research interests focus on materials for solid-state quantum information processing and their integration into hybrid quantum systems.

Christopher G. Yale received the B.S. degree in physics from Yale University, New Haven, CT, USA, in 2009 and the Ph.D. degree in physics from the University of California Santa Barbara, Santa Barbara, CA, USA, in 2015.

He is currently a Postdoctoral Scholar at the Institute for Molecular Engineering, University of Chicago, Chicago, IL, USA. His research interests include solid-state quantum information processing, quantum optics, and photonics.



David D. Awschalom (Member, IEEE) received the B.S. degree in physics from the University of Illinois at Urbana-Champaign, Urbana, IL, USA in 1978 and the Ph.D. degree in experimental physics from Cornell University, Ithaca, NY, USA in 1982.

He was a Research Staff Member and Manager at the IBM Watson Research Center, Yorktown Heights, NY, USA and later the Peter J. Clarke Professor of Physics and Electrical and Computer Engineering, and Director of the California Nano-Systems Institute at the University of California Santa Barbara, Santa Barbara, CA, USA. He is currently the Liew Family Professor in Spintronics and Quantum Information and Deputy Director in the Institute for Molecular Engineering, University of Chicago, Chicago, IL, USA and a Senior Scientist at Argonne National Laboratory, Argonne, IL, USA. His research activities focus on optical and magnetic interactions in semiconductor quantum structures, spin dynamics and coherence in condensed matter systems, and implementations of quantum information processing in the solid state.

Dr. Awschalom is a member of the National Academy of Sciences, the National Academy of Engineering, and the European Academy of Sciences.

